Cathodoluminescence petrography of Middle Proterozoic extrusive carbonatite from Qasiarsuk, South Greenland

CHRISTOPHER L. HAYWARD AND ADRIAN P. JONES

Department of Geological Sciences, University College London, Gower Street, London WC1E 6BT

Abstract

The amygdaloidal carbonatite lavas at Qasiarsuk have a primary phenocryst assemblage of calcite, fluor-apatite and magnetite set in a groundmass of calcite, apatite and iron oxides, and minor dolomite. Cathodoluminescence reveals a complex history, both for the major minerals which show zonal growth, and for important Nb and *REE* accessory phases which include pyrochlore and perovskite. The *REE* reside in fluor/hydrous-carbonates included exclusively in apatite. These *REE* minerals are similar to synthetic phases from hydrothermal experiments, but probably crystallised in equilibrium with a late-stage volatile-rich carbonate melt. Apart from low-temperature alteration, the rocks have been little disturbed since their extrusion during the earliest phase of development of the Gardar Alkaline Igneous Province.

KEYWORDS: cathodoluminescence petrography, carbonatite, Qasiarsuk, Greenland.

Introduction

MIDDLE Proterozoic carbonatite lavas from the Qasiarsuk (syn. Qagssiarssuk) area of South Greenland are amongst the oldest extrusive carbonatites known. This paper presents the first detailed description since the work of Stewart (1970). Petrographic textures revealed by cathodoluminescence studies, together with mineral and whole-rock analyses, are used to investigate their origin. They were originally described by Stewart (1970) and thought to be 'carbonated melilite rock'. Deans and Roberts (1984) used the same lavas to demonstrate their hypothesis that many calcium carbonatite lavas represent replaced and recrystallised natrocarbonatite lavas. Subsequently, Jones (1985) presented additional field data and Knudsen (1986) included apatite data in an economic assessment of Greenland carbonatites.

Geology

A sequence of Middle Proterozoic carbonatite volcanic rocks is preserved in a fault-bounded block (the 'Qasiarsuk Triangle'), at Qasiarsuk, near Narsarsuak in South Greenland (Fig. 1).

Their geology has been described by Stewart (1970), who suggested a simple structural relationship between intrusive 'monchiquites', fluidised pipe breccias and a south-easterly dipping succession of carbonatitic volcanics. Their age is imprecisely constrained between 1600–1300 Ma. Both the volcanic unit and the pre-1600 Ma basement are cut by 'tuffsite' diatremes and vents containing blocks of sövite, orthoclasite and country rocks in a matrix that varies from carbonatite and monchiquite to altered mica-peridotite (alnöite). The local gneissose basement is cut by numerous carbonatite and ultramafic lamprophyre dykes and sills (Upton and Emeleus, 1987). These strongly alkaline intrusions are associated by potassic metasomatism of the surrounding basement, and often surrounded by K-fenite.

The volcanic unit may be up to 375 m thick (Stewart 1970) and consists of thin, vesicular carbonatite lavas overlain by bedded and cross-bedded calcareous tuffs, including lapilli tuffs and agglomerates. Representative samples were collected from the best exposure near a 25 m raised beach. Here, up to 10 m of bedded red tuffs show graded bedding immediately overlying a 2 m thickness of vesicular lava, which represents at least two flow units.
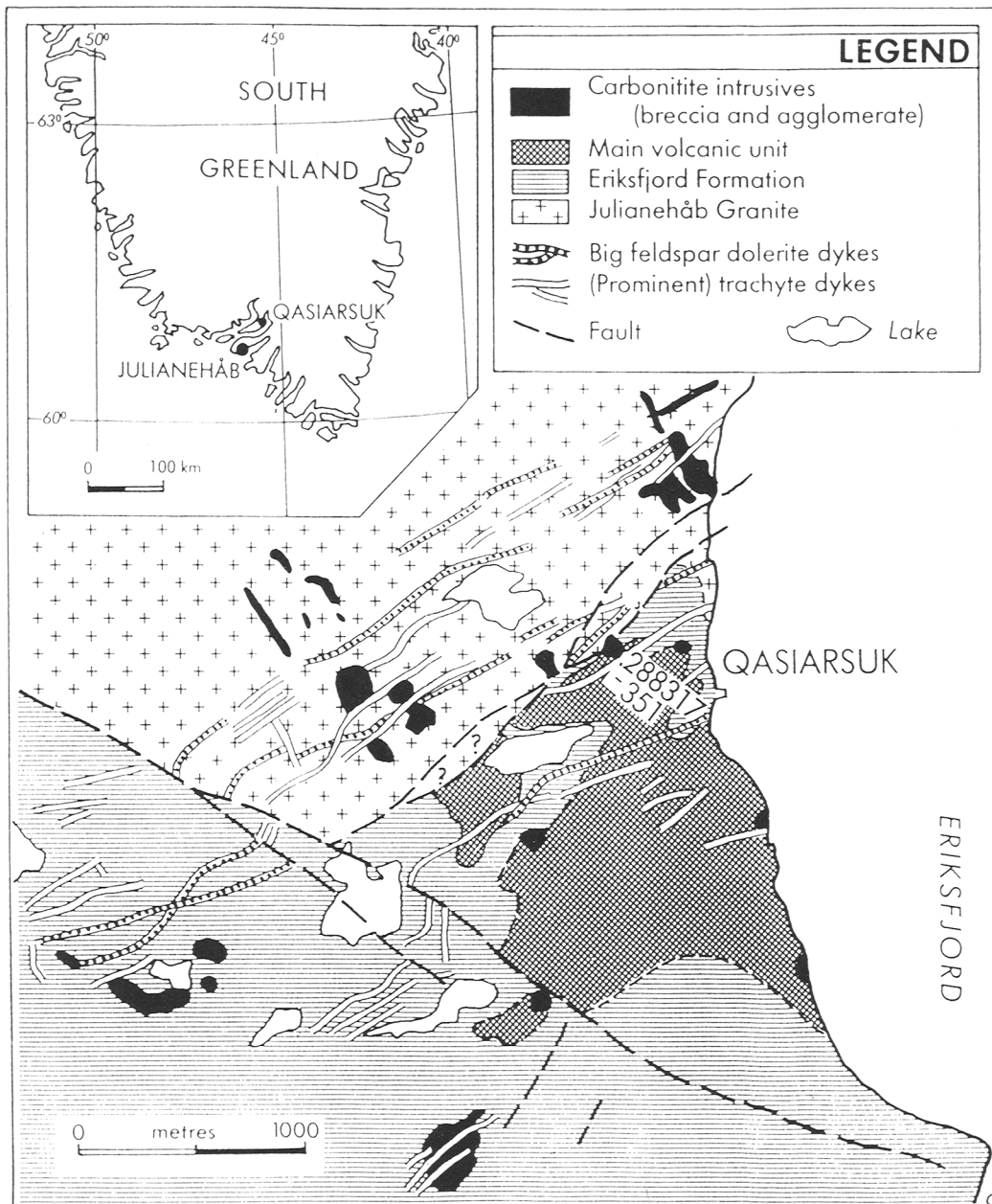
FIG. 1. Simplified geological map of the Qasiarsuk Triangle and surrounding area.

Two carbonatite lava samples from separate flows within the raised beach section were selected for study: 288317, a single probe section and 288351, from which six sections were cut. The samples were studied with transmitted and incident light mciroscopy, and cathodoluminescence (CL) microscopy using a Technosyn Cold Cath-ode Luminescence Model 8200 Mk.2. Photomicrographs were taken with a Nikon FX-35A camera with a Nikon UFX-2 automatic exposure unit using 400 ASA Fuji chrome film. Analyses were made with the Natural History Museum Hitachi S 2500 electron microprobe coupled with a Link AN-10 EDS X-ray analysis system.

General petrography

The textures and mineralogies of both samples are closely similar. Hand specimen 288351 is a reddish-brown colour, medium grained rock with many prominent, elongated, tubular amygdales which contain coarse, colourless calcite, and often pale yellow dolomite and occasionally baryte. The fresh groundmass 'sparkles' with numerous tiny (<1 mm) calcite laths and irregular grains which weather preferentially to give a finely pitted texture. Also present are occasional groups of pink, vitreous alkali feldspar xenocrysts.

The petrographic textures of these carbonatites are complex. It is clear that the rocks have experienced several different phases of crystallisation from magmatic through to low temperature hydrothermal conditions.

The microporphyritic volcanic texture of the lavas is recognisable, but has been substantially overprinted by polyphase, postmagmatic carbonate recrystallisation and replacement. Small calcite, apatite and relic accessory magnetite phenocrysts (0.05–0.4 mm) are set in a dark groundmass of microcrystalline calcite, apatite and microscopic globules of an iron-rich opaque phase, probably hematite; the latter gives the rock its distinctive red colour. Calcite laths comprise approximately 90% of the phenocryst assemblage. The phenocrysts are locally aligned over a few mm² but no definite trachytic texture exists. Additional irregular carbonate fragments (0.2 < 0.01 mm) and opaque grains occur in the groundmass and some of this calcite is locally dolomitised. Small subhedral to anhedral apatites, and quartz-apatite aggregates are common.

Highly altered accessory octahedral magnetites, 0.05–0.2 mm across, occur in isolation and glomeroporphyritically associated with apatite and calcite phenocrysts. Other minerals include altered niobium-rich phases after perovskite and pyrochlore, and occasional fresh perovskite inclusions, 0.1 mm across, are found in early-formed apatite phenocrysts (Table 5, Fig. 2).

Cathodoluminescence petrography

Cathodoluminescence (CL) is a useful petrographic tool (Marshall, 1988) and a particularly powerful technique with which to observe and interpret carbonatites. It reveals a vast amount of textural and compositional information invisible to normal optical methods. The Qasiarsuk carbonatites are particularly well suited to study by CL since both major minerals (calcite and apatite) luminesce. In the subsequent description of CL results, all colours, unless otherwise stated, refer
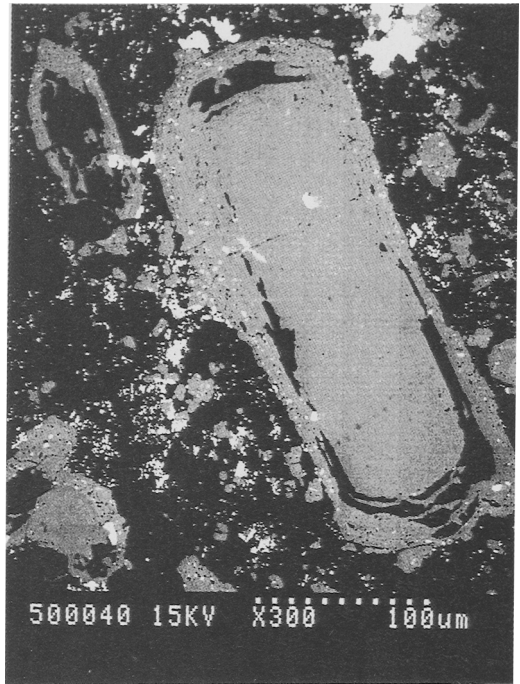

FIG. 2. Backscattered electron image of the zoned apatite phenocryst in Figs. 3 and 6. The fresh perovskite inclusion is the 30 μm white area in the central, upper part of the phenocryst, no other inclusions occur in the core. Small, white and black areas in the rim are RE-fluoro/hydroxy-carbonate and calcite/quartz inclusions respectively. Quartz plus dolomite ring is broken up by thin violet apatite screens, especially at terminations.

to luminescence colours. Elements which cause luminescence are called 'activators', and those which prevent luminescence are called 'quenchers'. The levels of these activators and quenchers are well below the detection limits of the EDS microprobe. See Table 1 for an explanation of CL colours.

The luminescence intensity of the carbonates (orange and deep red to red-orange for calcite and dolomite respectively), is controlled by the relative proportions of trace iron and manganese (Pierson, 1981), expressed here as relative Mn/Fe ratios, hence nonluminescent carbonate has relatively low Mn/Fe. It should be noted that identical-looking CL in calcite could be produced by crystallisation from fluids with different absolute manganese and iron concentrations, but very similar Mn/Fe. Therefore conclusions about relative times of crystallisation should be made with caution when unsupported by other evidence. In the Qasiarsuk carbonatite, calcite occurs in a variety of textural forms: phenocrysts, amyg-

MINERAL	ACTIVATOR	QUENCHER	COLOUR OF LUMINESCENCE
Calcite	Mn^{2+}	Fe^{2+}	Orange[1]
Mn-bearing calcite	Mn^{2+}	Fe^{2+}	Bright yellow to yellow-orange
Dolomite	Mn^{2+}	Fe^{2+}	Red-orange to deep red
Apatite	Eu^{2+}	-	Blue ⎫ ⎬ Violet[2] Red ⎭
	Eu^{3+}	-	

[1] Pierson (1981). [2] Mariano and Ring (1975) note that combination of blue and red emissions gives violet luminescence.

dales, groundmass and as veinlets cross-cutting these. The calcite may be sparry in nature, polycrystalline or microcrystalline.

The blue apatite luminescence is caused by Eu^{2+} and red-luminescing Eu^{3+} (Mariano and Ring, 1975). Mariano (1988), states that 'the strong blue emission frequently observed in carbonatite apatites may be due mainly to a structural defect produced by anomalous amounts of Sigma *REE* substitution for Ca^{2+} in the structure'. However no *REE*s were detected in the apatites other than those present in the RE-mineral inclusions (see below), which apparently rules out this explanation of the blue luminescence.

It should be remembered that the identification of activators through luminescence colour alone can in some cases be risky as there may be more than one possible explanation for a luminescence colour in a particular mineral. However the luminescence characteristics of the apatite and carbonates reported here have been previously documented by several authors (see below for references), and we feel that this evidence justifies the assignment of activators in the present work.

Phenocrysts

Calcite. The calcite phenocrysts vary in length from 0.2 to 0.7 mm but are usually 0.3–0.4 mm long and composed of sparry calcite or microcrystalline carbonate dusted with microscopic hematite grains. Terminations are commonly rounded, but more euhedral morphology is preserved especially in the sparry calcite laths (Fig. 3), which display several forms. Sparry calcite is essentially nonluminescent except for weakly

luminescent twins. Occasionally seen are groups of four or five sparry or polygranular laths, radiating from a point in a cross-like fashion.

In sample 288317, the calcite phenocrysts are composed mainly of pale microcrystalline calcite dusted with hematite, and is partially dolomitised. Colourless, opaque-free polygranular sparry calcite phenocrysts are less common and have rims recrystallised to the same microcrystalline calcite and opaque grains. Recrystallised, microcrystalline margins of sparry calcite grains, discernible by normal microscopy are indistiguishable from the groundmass in CL. The calcite phenocrysts in sample 288351 are mostly composed of sparry calcite, either as single crystals, or more commonly as polycrystalline aggregates. Sparry calcite phenocrysts often have small opaque aggregates at their margins which form a discontinuous rim, the margins may also be corroded. The calcite phenocrysts have an almost pure composition distinct from the other carbonates in the rocks. They closely resemble similar calcite phenocrysts in extrusive carbonatites from Kaiserstuhl (Tuttle and Gittins, 1966; Keller, 1989), and Kerimasi (Mariano and Roedder, 1983).

Apatite. Much of the apatite (4–5% mode) forms euhedral to subhedral prismatic phenocrysts 0.05–0.2 mm long and up to 0.4 mm in sample 288317. In plane-polarised light, the apatites typically have colourless cores and clouded red–brown to dark brown coloured rims, which invariably contain abundant tiny crystalline inclusions, which are scattered randomly or form coreconcentric rings or rarely couble rings. CL reveals several types of core-rim-inclusion relationships (Fig. 4), and also the widespread presence of small subhedral to anhedral violet apatites dispersed throughout the opaque-rich groundmass. Electron microprobe analyses indicate that these inclusions consist of calcite, dolomite, *RE*-carbonates, *RE*-phosphate and quartz. Several apatites have cores separated from rims by a semi-continuous band of quartz 5–10 μm in width (Figs. 2, 4, 6).

Apatite phenocryst cores luminesce bright blue and often show oscillatory zoning with bands of differing intensity blue. This zoning is usually concentric but can be complex with zoning nonconcentric with the phenocryst margin. Multistage core growth and resorbtion is seen with earlier concentric zones uncomfortably overgrown by later zones (Fig. 5). The blue cores have rims of violet apatite and the margins of the cores may be darker blue adjacent to the violet rims. The rim inclusions luminesce as follows: calcite — orange; Mn-bearing calcite — yellow; and
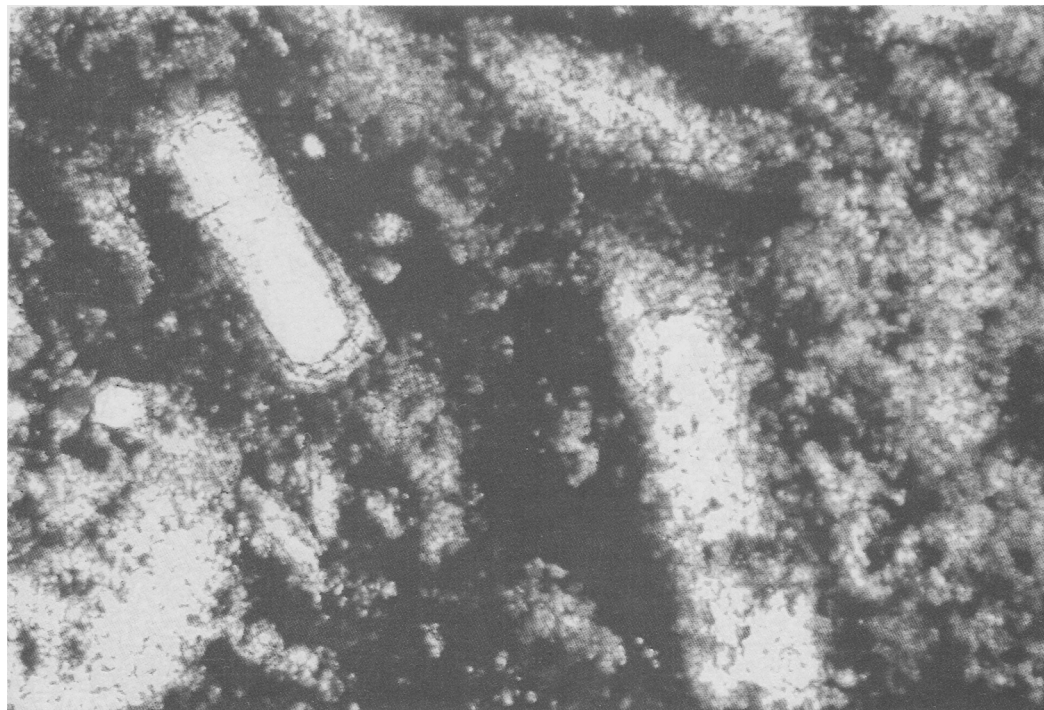
FIG. 3. Plane-polarised light photomicrograph of Fig. 6. Note the far greater detail visible in cathodoluminescence. The largest phenocryst is calcite, the paler ones are apatite.

quartz—dark purple. Relatively high manganese contents (0.9–1.9 wt.% MnO), in comparison with all other calcite (0.2–0.5 wt.% MnO), coincides with the yellow luminescence of some calcite inclusions. The low-intensity quartz luminescence is usually swamped by the stronger calcite and apatite luminescence. Backscattered electron imagery reveals many more inclusions, not visible in CL. The quartz bands partially enclose some cores and are best developed at crystal terminations where they may be divided into very narrow bands separated by thin screens of violet apatite 5 μm or less thick. In one large phenocryst (type 1a, Figs. 2, 4 and 6), a nonluminescent dolomite band occurs nearest the core.

Inclusion rings usually follow the form of the blue cores irrespective of rim morphology. All cores are entirely free of these inclusions. The violet rims may preserve the original euhedral, prismatic shape of the blue core, or mimic the present core form, subhedral or otherwise, like an overgrowth. Rounded core relics may be 'off-centre' with respect to the surrounding violet rim. Occasionally, small (0.05 mm) euhedral or subhedral blue apatites occur at one end of a much larger subhedral violet grain or multigranular

aggregate, for which it appears to have acted as a nucleation point.

Profiles were analysed by electron microprobe across a variety of apatite types. The results, (Table 2) show that all apatites are compositionally very similar. Strontium is the only commonly detected impurity (0.4–1.2 wt.% SrO). Silicon occurs in several analyses (0.25–1.3 wt.% SiO_2). The Ca/P ratio for almost all apatites is 1.28–1.30 and remains relatively uniform for individual apatites. Irregular variation between 1.26 and 1.76 occurs mostly in larger, type 1 (Fig. 4) phenocrysts. Groundmass apatites have slightly higher values of 1.31–1.33 which is probably an analytical artefact and reflects beam overlap onto groundmass carbonates.

Strontium usually decreases from the centre to the margin of the blue cores. Dark blue bands have slightly lower levels of strontium. Violet rims generally have different Sr levels to the cores, either higher or lower and a relatively large perturbation in Sr is common at the blue–violet interface (Fig. 8). Identical Sr variation occurs in violet apatites without blue cores.

In sample 288317, microcrystalline granular apatite associated with opaque-rich groundmass
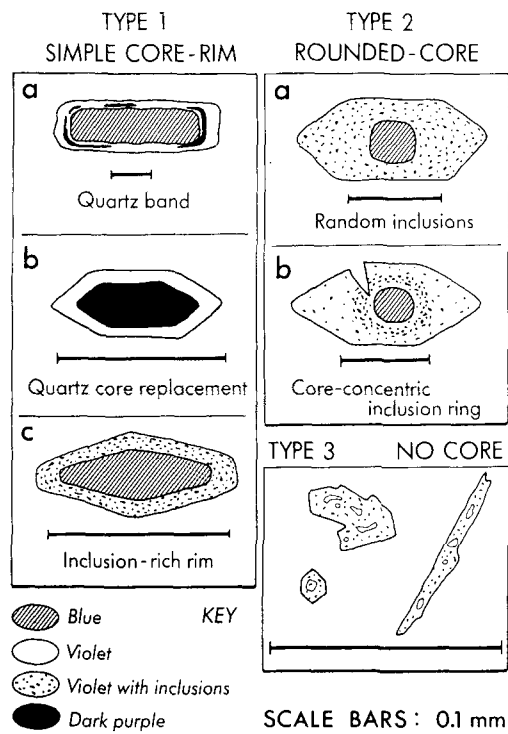
TYPE 1
SIMPLE CORE-RIM

a

Quartz band

b

Quartz core replacement

c

Inclusion-rich rim

KEY

Blue

Violet

Violet with inclusions

Dark purple

TYPE 2
ROUNDED-CORE

a

Random inclusions

b

Core-concentric
inclusion ring

TYPE 3   NO CORE

SCALE BARS: 0.1 mm

FIG. 4. Classification of apatites from the lava samples based on relationships between core, rim and inclusions in cathodoluminescence.

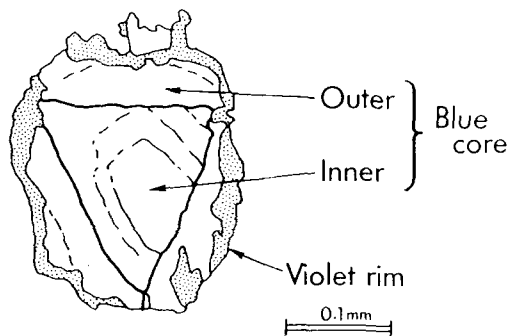Outer ⎫
        ⎬ Blue
Inner ⎭   core

Violet rim

0.1mm

FIG. 5. Complexly zoned apatite phenocryst in cathodoluminescence showing multiple growth and resorbtion episodes (sample 288351).

areas is intergrown with quartz and less abundant Mn-bearing calcite. In both samples the most abundant form of apatite occurs as numerous, small (<0.1 mm), euhedral to anhedral unzoned violet grains. These usually contain many inclusions (calcite, RE-carbonate(s), quartz), of which

the larger ones (approximately 0.1 mm) may be polyphase and occupy substantial areas of the apatite grain (type 3, Fig. 4). In sample 288317 and less commonly in 288351, violet apatites (0.2– <0.05 mm) may have dark purple quartz cores which occsionally have yellow Mn-bearing calcite inclusions. One violet apatite has a core of Mn-bearing calcite alone. These type 3 apatites occur singly and as polycrystalline groups. The smallest apatites occur as irregular aggregates of tiny (<0.005 mm) grains associated with opaque-rich areas at amygdale margins and in the ground mass.

Rare earth minerals. At least two rare earth (RE) minerals occur as inclusions in violet apatite. Because of their small size they have not been positively identified. However, from consideration of their stoichiometry (Table 3 partial analyses) by far the most abundant phase appears to be a fluoro/hydroxy-calcium-RE-carbonate. The presence of fluorine is implied from the analyses of fluorapatites from Qasiarsuk (Knudsen, 1986), and the presence of OH^- is implied from the low analytical totals. This is consistent with the volatile-rich conditions that are likely to have prevailed during crystallisation of these phases. The stoichiometry of this phase is unlike the common RE-fluoro-hydroxy-carbonates of the bastnaesite–synchisite mixed-layer compounds (e.g. Jones and Wyllie, 1985), and resembles synthetic, hydrothermal RE-phases (Chai and Mroczkowski, 1978, and references therein). The phase shows limited variation in La:Ce ratios, and near constant Nd (Fig. 8).

The second and far less abundant RE-phase is a RE-phosphate whose stoichiometry closely resembles monazite. Chondrite-normalised RE abundances (Nakamura, 1974) for all of the RE minerals show extreme light-RE enrichment, very similar to whole rock RE distributions for these and other Qasiarsuk samples, measured by XRF analysis (this work, Fig. 9). Such light-RE enrichment is characteristic of carbonatites in general.

Nonphenocrysts

Amygdales. The generally nonluminescent sparry calcite grains in amygdales, veins and the groundmass fragments often have concentric, bright orange growth bands, 0.1–0.001 mm wide. Thicker bands may be made up of many narrower orange and nonluminescent bands. The bands reveal complex growth and resorption histories for some calcite grains. In amygdales, identical bands occur in separate grains, which indicates contemporaneous growth from evolving fluids. In some amygdale carbonate grains, the bands pass
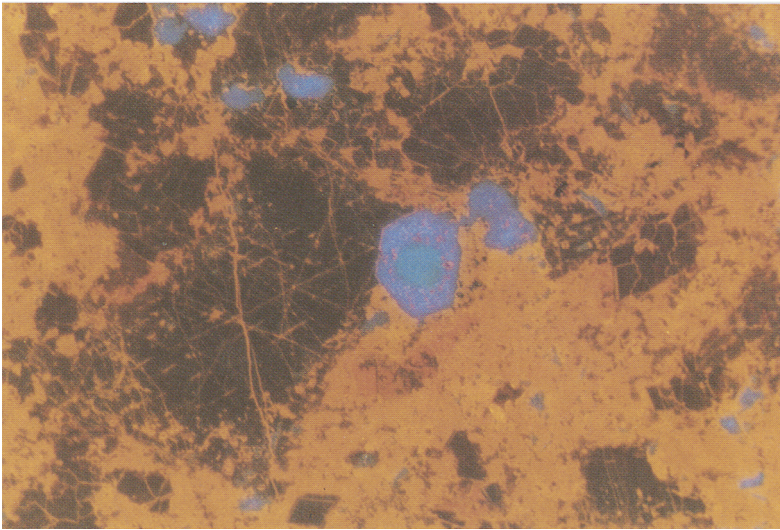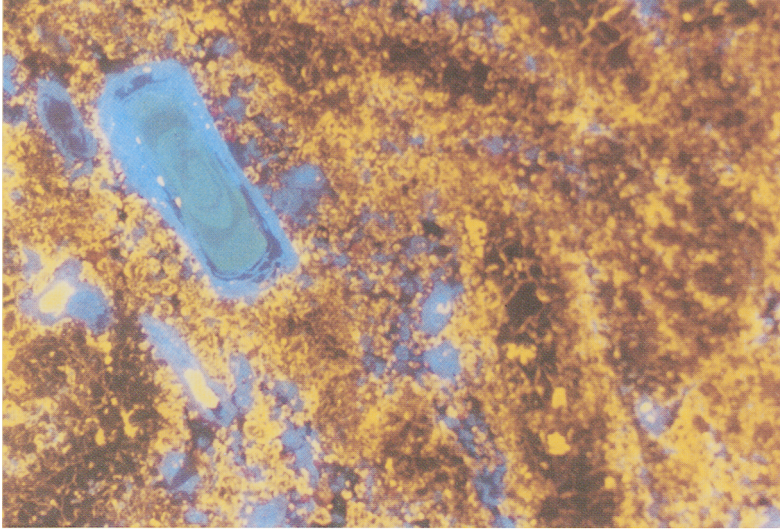
FIGS. 6 and 7. FIG. 6 (*top*). Type 1a and 1b apatite phenocrysts and surrounding carbonate groundmass. Type 1a: concentric zoning in blue core and dark silica plus dolomite band separating blue core and violet rim. Type 1b: violet luminescence with quartz and Mn-bearing calcite cores. Carbonate groundmass has non-luminescent sparry fragments within younger, orange microcrystalline calcite. Rims of nonluminescent calcite phenocrysts are replaced by luminescent, microcrystalline calcite. Field of view 2 mm. (Sample 288317.) FIG. 7 (*bottom*). Glomeroporphyritic growth of a type 2a apatite on a nonluminescent calcite phenocryst. Note the orange veinlets cutting nonluminescent calcite. Field of view 2 mm. (Sample 288351.)

continuously across boundaries between grains of different crystallographic orientation, with a corresponding change in direction.

Dolomite occurs as small (0.01 mm), red euhedra in the core regions of many amygdales, and also preferentially replacing some growth bands in the calcite grains. Nonluminescent, subhedral to anhedral barite occurs in some amygdales, some barite grains exhibit fluid inclusion-rich subhedral cores enclosed within fluid inclusion-poor rims.

Amygdale calcite contains low levels of both

	1	2	3	4	5	6	7
CaO	53.8	54.1	53.9	53.7	53.7	54.1	52.3
SrO	0.88	0.82	0.91	1.16	1.02	0.44	0.52
P_2O_5	42.1	42.2	41.7	42.0	41.7	42.2	39.3
SiO_2	n.d.	n.d.	0.36	1.28	n.d.	n.d.	1.22
TOTAL	96.78	97.12	96.87	98.14	96.42	96.74	93.34

1-4 phenocryst type 1. Luminescence bright blue or dark blue.
5-6 phenocryst type 3. Microphenocryst, luminescence violet.
7 phenocryst type 3. Groundmass grain, luminescence violet.
n.d. not detected. (RE_2O_3= 0.23-0.30 wt%, F= 3.10-4.40 wt%, Knudsen, 1986).

MgO (0.2–0.5.wt.%), and occasionally strontium (up to 0.4 wt.% SrO). Iron (FeO) is below detection in all analysed amygdale calcite. Dolomite in amygdales also contains strontium (0.4 wt.% SrO), and some manganese (0.2 wt.%).

The amygdales are rimmed by a thin opaque-rich band 0.1–0.2 mm wide, which contains calcite fragments and subhedral to globular apatites (<0.05 mm), visible only in CL. Amygdale calcite grains do not traverse the opaque rim into the groundmass. Surrounding the amygdales are 0.3–1.5 mm wide areas of pale groundmass, poor in opaque micrograins and dominated by sparry calcite. This pale groundmass becomes gradually richer in microscopic opaques further from the amygdales before an abrupt transition occurs to the normal, dark groundmass.

Recrystallisation of the groundmass around some amygdales to large poikilitic, sparry grains several mm across has occurred. These sparry grains overgrow and preserve the pre-existing included textures and grains, and are best developed adjacent to the amygdales.

Groundmass. The dominant groundmass mineral is calcite, with dolomite far less abundant. Both groundmass carbonates contain similar levels of MgO and SrO to amygdale carbonates. FeO levels could not be determined accurately because of analytical overlap with the abundant dispersed hematite particles.

In CL the groundmass carbonate is essentially nonluminescent and composed of numerous angular to subrounded calcite fragments, cemented in younger orange calcite, which is dominant in some areas. Many of these fragments probably derive from broken phenocrysts. The orange groundmass calcite cement appears to have recrystallised from previous fine-grained carbonate. Several generations of carbonate veinlets can be distinguished by crosscutting relationships and differing intensities of CL. Early, nonluminescent veins with fragments of orange calcite are cut by random, narrower (0.01–

0.001 mm), more numerous orange calcite veinlets which cut calcite phenocrysts, amygdales and groundmass (Fig. 7). The youngest orange veinlets do not cut, and are sometimes overgrown by the even younger anhedral and globular apatites of type 3. These veinlets have been partially dolomitised with the surrounding groundmass; they become indistinguishable where they enter the bright orange groundmass and are invisible by normal microscopy. Occasional braided, bright orange relatively wide veins (0.2 mm), are just visible in plane-polarised light. These cut and are themselves overgrown by different generations of violet apatites. Less common, narrower dull orange veins cut the bright veins.

Some relatively extensive areas of bright orange sparry calcite contain angular fragments of orange, growth-banded, nonluminescent calcite (Fig. 10). The orange calcite surrounding these nonluminescent fragments may be concentrically banded in various intensities of orange parallel to the fragment edges which indicates a cavity-filling relationship with the pre-existing nonluminescent calcite. In plane-polarized light, all the calcite is optically continuous with no indication of this texture.

Crystallisation events

The combined use of optical petrography and CL has revealed a complex crystallisation history for these rocks. An attempt is now made to rationalise the textures in conjunction with analysed mineral compositions in a sequence of events which have effected the rocks. Further, detailed trace chemcial variations are inferrred from established relationships between CL and luminescence activators (Table 1).

Calcite. The CL technique shows several generations of calcite crystallisation. Calcite with relatively low Mn/Fe (non-luminescent) forms both the phenocrysts, some of which are fragmented, and the amygdales. Orange growth bands in the non-luminescent amygdale calcite indicate icnreases in Mn/Fe of the mineralising melt(s)/fluid(s). Sharp edges to many bands indicate that these changes occurred rapidly with respect to calcite growth rates. As previously observed, banding occurs on several scales from 0.1 to 0.001 mm. Thick orange bands made up of many thinner bands of varying luminescence intensity show that minor, short-lived fluctuations in fluid chemistry occurred during overall periods of higher Mn/Fe calcite growth. Such growth banding may also be present in the non-luminescent calcite, including phenocrysts, but is not visible because of quenching by low Mn/Fe.
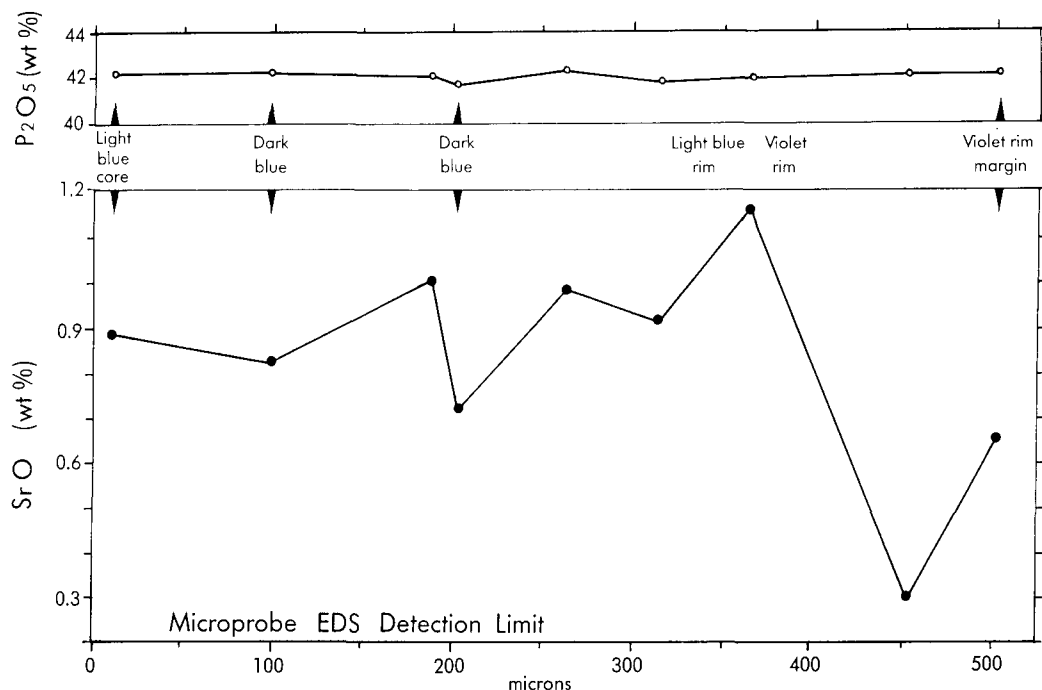
FIG. 8. EDS electron probe core-to-rim traverse of the upper half of the zoned, type 1a phenocryst in Figs. 2, 3 and 6. Apatite analyses shown only.

TABLE 3. PARTIAL ANALYSES OF REE MINERAL INCLUSIONS IN APATITES.

	1	2	3	4
P_2O_5	n.d.	0.39	2.07	n.d.
SiO_2	n.d.	0.43	4.53	0.86
ThO_2	n.d.	1.18	n.d.	n.d.
Al_2O_3	n.d.	0.42	n.d.	0.25
FeO	n.d.	0.42	n.d.	0.95
CaO	17.36	17.50	15.28	14.76
SrO	0.32	0.56	0.87	0.59
La_2O_3	16.35	10.91	13.02	5.41
Ce_2O_3	22.38	20.46	26.01	37.72
Pr_2O_3	2.00	1.98	1.16	1.01
Nd_2O_3	7.02	8.52	5.40	4.17
Sm_2O_3	n.d.	0.88	n.d.	n.d.
Y_2O_3	n.d.	0.53	n.d.	n.d.
TOTAL	63.43	62.76	68.34	65.72

1-3: Ca-RE-fluoro/hydrous-carbonate; note the thorium in 2.
4 : Ce-rich variety of fluoro/hydrous carbonates.
n.d.= not detected. Fluorine not analysed for, but is inferred from coexisting fluor-apatite, (Knudsen, 1986)

Calcite growth in the amygdales was evidently discontinuous since some orange growth bands are clearly resorbed.

The pale calcite areas surrounding the amygdales crystallised at the same time as large ophitic sparry grains which enclose the groundmass grains and textures. Colourless calcite zones around amygdales are consistent with local transport of iron from the calcite, to form the dark, iron-rich rims to the amygdales.

Orange calcite in both veins and groundmass is often continuous and indistinguishable, and hence possibly contemporaneous. The introduction of the orange calcite has been associated with recrystallisation and fragmentation of the pre-existing, nonluminescent calcite (Figs. 7, 10). It is not clear when the orange calcite inclusions in apatite formed.

The reasonable degree of textural preservation seen in these lavas suggests that any replacement was acheived at near constant volume. This probably precludes extensive replacement of primary Na- and K-carbonates (nyerereite, gregoryite) by Ca-carbonate, since this would lead to large volume reductions of up to 42% (Deans and Roberts, 1984). The morphology of the calcite phenocrysts closely resembles those at Kaiserstuhl, Germany (Tuttle and Gittins, 1966; Keller, 1989), and Kerimasi, Tanzania (Mariano and Roedder, 1983) which show concentric growth
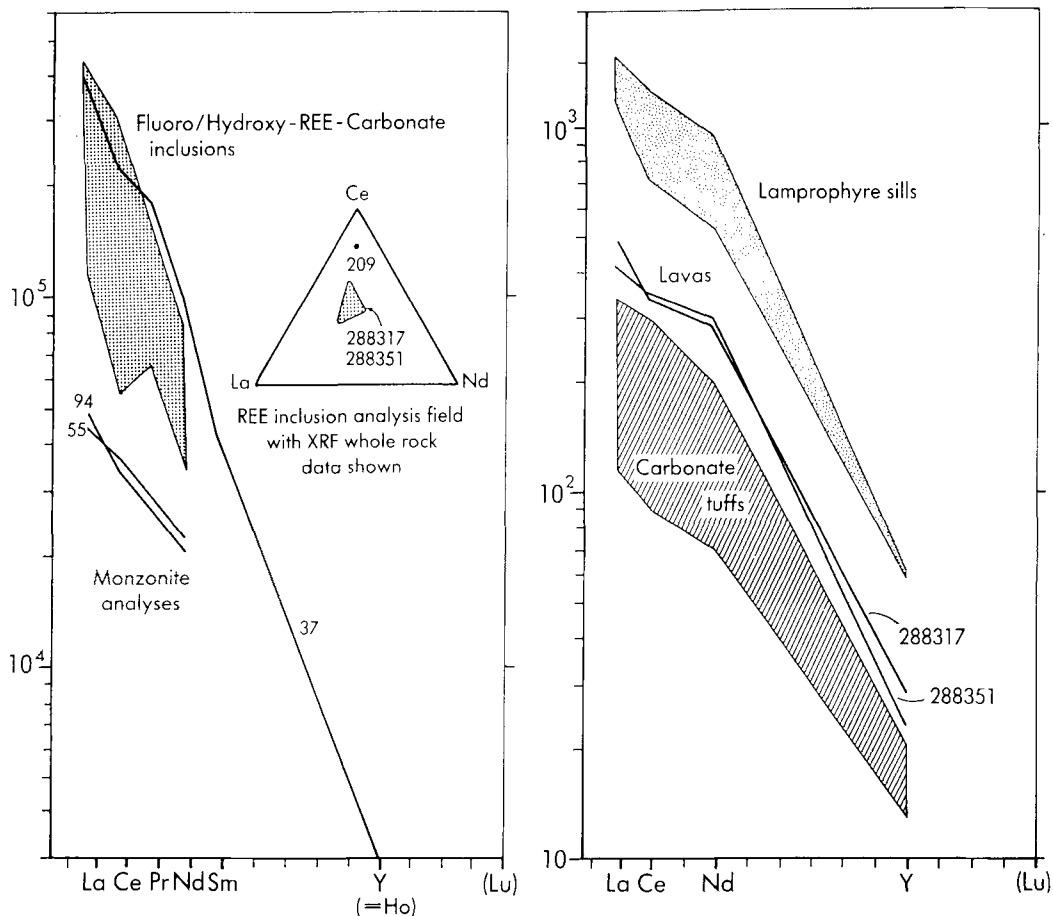
FIG. 9. *REE* diagrams of (*a*) apatite *RE*-fluoro/hydroxy-carbonate and monazite inclusions and, (*b*) XRF whole-rock analyses of the carbonatite extrusives and associated ultramafic lamprophyre dykes from the Qasiarsuk area.

TABLE 4. CARBONATE PARTIAL ANALYSES.

	1	2	3	4	5	6	7
SiO_2	0.19	0.14	0.21	0.16	n.d.	n.d.	0.19
P_2O_5	n.d.	0.25	n.d.	n.d.	n.d.	n.d.	0.40
SrO	n.d.	0.25	0.40	n.d.	0.30	0.37	n.d.
CaO	53.8	53.3	52.7	52.4	53.6	31.5	32.5
MgO	n.d.	0.28	0.36	0.43	0.25	18.8	16.6
MnO	n.d.	n.d.	0.38	1.88	n.d.	n.d.	0.34
FeO	n.d.	n.d.	n.d.	n.d.	n.d.	n.d.	0.34
TOTAL	53.99	54.22	54.05	54.87	54.15	50.86	51.67

1= phenocryst calcite core;   2= nonluminescent amygdale calcite;
3= inclusion in violet (CL) apatite core;   4= yellow (CL) calcite inclusion in violet apatite core;
5= groundmass calcite;   6= dolomite centre of amygdale, red (CL);
7= dolomite, yellow-orange (CL) in violet rim of type 1 apatite.
n.d.= not detected.

zoning in CL. Although the calcite phenocrysts in the Qasiarsuk lavas do not exhibit growth zoning in CL, all other features are consistent with their having crystallised from primary calcium-carbonatite magmas (zoning may be present, but CL activator concentrations are too low to produce luminescence).

The lowest temperature event is recorded by the microscopic hematite globules (dusting), in the groundmass, and iron-rich concentrations at the rims of amygdales and sparry calcite phenocrysts, which are probably the result of *in situ* postmagmatic hydrothermal oxidation (Anderson, 1986). The volumetrically minor quantity of hematite does not require significant metasomatic enrichment. Instead however, the textural association with recrystallisation of groundmass calcite, and corrosion of sparry calcite suggests that the source of the iron was pre-existing FeO in calcite and magnetite, which is abundant in many of the tuffs (Stewart, 1970; Deans and Seager, 1978).
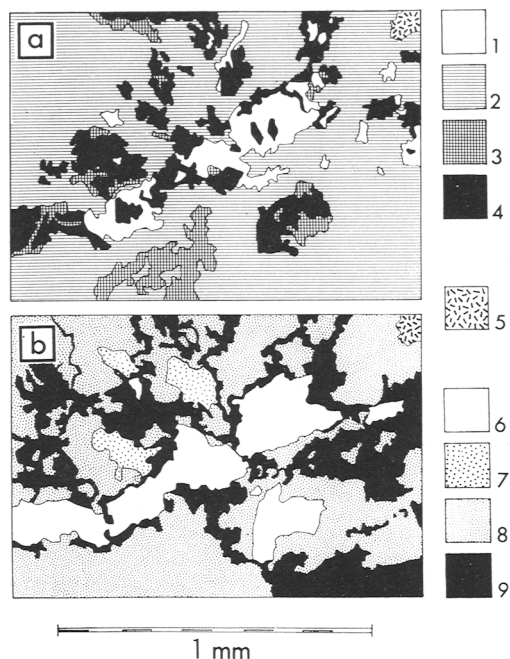
Dolomite in amygdales, veinlets and the

FIG. 10. Sparry calcite vein in (*a*) cathodoluminescence, (*b*) plane-polarised light, showing fragmentation and displacement of older non-luminescent by younger, orange-luminescent sparry calcite. Sparry vein calcite is optically continuous and hence this texture is invisible in plane-polarised light. Drawn from photomicrographs, sample 288351. KEY: 1, intense orange luminescence; 2, bright orange luminescence; 3, dull orange; 4, nonluminescent; 5, apatite; 6, colourless sparry calcite; 7, sparry calcite with light opaque dusting; 8, heavily dusted microcrystalline calcite; 9, opaque-dominated microcrystalline carbonate(s).

groundmass is a late-stage replacement of calcite, based on the overprint textures.

Apatite. The CL of the apatites is complex and varied. Eu^{2+}-activated blue patite is always surrounded by a rim of Eu^{2+} and Eu^{3+}-activated apatite, which they clearly predate. Eu^{2+} is a sensitive indicator of reducing conditions (Goldschmidt, 1958), which may exist in carbonatitic magma chambers, and probably indicates a magmatic origin for at least the blue apatite. The luminescence reveals concentric and complex zoning (a common magmatic feature), with bands of darker blue (strontium-poor) in normal bright blue apatite.

Violet apatites may have been formed by either (1) secondary partial oxidation of Eu^{2+} to Eu^{3+} from the rim inwards, or (2) later overgrowth of violet apatite on blue, in an oxidising environment. Secondary oxidation is unlikely, however, to have been the main source of violet apatite

formation since the CL colours and zones are not influenced by cracks in apatite grains which would have provided passage for the oxidising melts and/or fluids. Also, blue cores do not contain the expected inclusions of carbonates and silica as found in the violet apatite if the latter formed by secondary oxidation. Blue cores are conspicuously free from these inclusions. Finally, there is a break in the strontium content at the core-rim boundary. The rounded blue apatites therefore were apparently resorbed in a melt/fluid prior to the onset of increasingly oxidising conditions. The occurrence of a rounded blue apatite with two unconformable, concentrically zoned regions, the outer truncating the inner (Fig. 5), supports the idea of discontinuous growth. In this particular grain, the outer blue zoned region has itself been resorbed before growth of the violet rim.

The violet rims and iolated violet apatites are interpreted to represent growth in oxidising conditions. Their euhedral or subhedral textures are consistent with growth in a melt and/or fluid environment which allowed the development of crystal faces. They are compositionally indistinguishable from the blue apatites, except for lower strontium in some rims. Examples of inclusion-rich, euhedral violet apatites with or without blue cores, glomeroporphyritically associated with calcite phenocrysts indicates their early growth from a melt (Fig. 7). Some anhedral violet apatites are undoubtedly of late hydrothermal origin since occasionally they overgrow the latest generation of orange calcite veinlets. Violet apatite growth therefore apparently continued through the magmatic and hydrothermal history of the lavas.

Inclusions within violet apatites of Mn-bearing calcite, *RE*-carbonates, silica and monazite indicates mobility of Mn, *LREE*, and Si and their presence in melts and/or fluids during violet apatite growth. None of these included phases are found isolated from violet apatite. The inclusion-forming components were not uniformly present with respect to concentration or time. Inclusions, dominated in number by calcite and Mn-bearing calcite, commonly form single inclusion rings within the violet apatite or rarely double rings. This indicates fluctuation in inclusion formation rate and punctuation of apatite growth. Changes in the rate of inclusion growth apparently occurred since rather large, sometimes polyphase inclusions occur in both isolated apatites and are also common as the main component in some inclusion rings. The mineral and phase chemistry of the inclusions is rather consistent and simple, suggesting rapid diffusion in the parental melt or fluid.

TABLE 5. NIOBIUM MINERALS.

	1	2	3
Nb_2O_5	61.5	37.9	46.1
SiO_2	0.41	0.39	0.45
TiO_2	6.30	39.0	22.4
FeO	n.d.	21.1	28.5
MnO	n.d.	0.39	0.53
CaO	20.75	0.36	0.37
SrO	0.42	n.d.	n.d.
Na_2O	3.99	n.d.	n.d.
TOTAL	93.97	99.14	98.35

RECALCULATION ON THE BASIS OF 6 OXYGENS.

Nb	1.572		0.852		1.123		
Si	0.023	1.86	0.019	2.33	0.024	2.05	
Ti	0.268		1.459		0.907		
Fe	0.000		0.877		1.284		
Mn	0.000		0.016		0.024		
Ca	1.257	1.71	0.019	0.91	0.021	1.33	
Sr	0.014		0.000		0.000		
Na	0.437		0.000		0.000		

1= perovskite inclusion in a type 1 apatite.
2= niobian grain in a Nb-Fe-rich aggregate (pseudomorph after pyrochlore or colombite).
3= niobium-rich micrograin in 2.

P, Al, Mg, Ba all below detection. REE probably present but below detection, (EDS analyses).

Rare earth minerals. The *REE* minerals are volatile-bearing carbonates occurring exclusively as inclusions in apatite. Analogous fluor/hydrous *REE* minerals are known from hydrothermal experiments (Chai and Mroczkowski, 1978), but may also form from vapour-saturated carbonate melts, at temperatures of approximately 500–600 °C (Jones and Wyllie, 1985). The transition between melt-present and fluid-dominated conditions represents the traditional crossover between classic igneous crystallisation and hydrothermal 'alteration' and mineralisation. For carbonatites in particular, where melts can dissolve very high volatile contents (>30 wt.%, Jones and Wyllie, 1985), this transition is likely to be complex, and to represent a continuum. The distribution of *REE* and nature of the *REE* host will simply reflect *REE*-phase stability. Experiments show that in addition to temperature, pressure and bulk composition, one critical parameter is the CO_2/H_2O ratio. The fluorine content is probably also important. Certainly carbonatite melts can dissolve major amounts of *LREE* (Jones and Wyllie, 1985), and the petrographic textures suggest that the euhedral apatites, which include the *REE*-carbonates, probably crystallised in equilibrium with a melt. For *REE* minerals crystallised during melt-absent conditions, the *REE* were probably transported as complexes with CO_2^{2-} and F^- in hydrothermal

or carbothermal (CO_2-dominated) solutions. They are strongly *LREE*-enriched, which reflect the lower solubility of *LREE* complexes compared to *HREE* complexes in fluids (Kosterin, 1959). The main factors influencing the stability of *REE* complexes in fluids and minerals are temperature and the alkalinity of the fluids. A temperature decrease from 400 °C to 100 °C at a constant pressure of 400 bars causes an increase in calcite solubility from 0.1 to several hundred mg dm^{-3}. Similar increases in *LREE* solubility occur at even lower temperatures of 100–200 °C. Alkalinity decreases, possibly due to loss of CO_2 or by carbonate crystallisation or devolatilisation (Kosterin, 1959) have the opposite effect, and promotes *REE*-mineral formation (Balashov and Pozharitskaya, 1968).

Close similarity between *REE* distribution patterns for individual inclusions and whole rock analyses shows that the *RE*-carbonate and monazite mineral inclusions effectively control the *REE* distribution in the rocks. If *RE* or other inclusion phases ever formed in isolation from the apatite then they have been subsequently removed.

Conclusions

Cathodoluminescence reveals a large amount of textural data which otherwise would have been missed. In particular, spectacular growth zoning and luminescence colours in apatite allow differentiation between successive generations, and interpretation of the chemistry and oxidation state of the evolving melt and fluids. Widespread recrystallisation of the carbonate minerals, and late-stage veining has occurred, but has not obscured the primary volcanic textures. The *REE* are strongly *LREE*-enriched, and apart from traces of monazite, are contained exclusively in volatile-bearing (fluor/hydroxy-) Ca-carbonbate inclusions within violet-luminescing apatite. Although details of the melt/fluid chemistry are not known, there is compelling evidence for the presence of fluorine (Knudsen, 1986), and hydrous components (Chai and Mroczkowski, 1978). Niobium mineral breakdown products after perovskite and pyrochlore are also present together with occasional fresh perovskite included in apatite phenocrysts.

The carbonatite lavas at Qasiarsuk are interpreted as calcium carbonatites with phenocrysts of calcite, apatite, magnetite, perovskite and pyrochlore. They have a chemistry (Jones, unpublished data) and mineralogy typical of calciocarbonatites worldwide (Woolley and Kempe, 989). We find no supporting evidence for

their having originally been either alkali-rich (Deans and Roberts, 1984), or melilite-bearing (Stewart, 1970). The Qasiarsuk sequence of Middle Proterozoic extrusive carbonatites is closely similar to Miocene calciocarbonatite volcanics from Kaiserstuhl (Tuttle and Gittins, 1966; Keller, 1989), including the association with lapilli tuffs. There is a large and rapidly increasing body of chemical data on extrusive carbonatites. The Qasiarsuk sequence provides an important ancient equivalent to the younger examples so far studied, which has been preserved in an unde-formed state and is now exposed at eruption level.

References

Anderson, T. (1986) Model for the evolution of haematite carbonatite based on whole rock major and trace element data from the Fen Complex, SE Norway, *Appl. Geochem.*, **2**, 163–80.

Balashov, Yu, A. and Pozharitskaya, L. K. (1968) Factors governing the behaviour of rare-earth ele-ments in carbonatitic processes. *Geochimiya*, **3**, 285–303.

Chai, H. T. and Mroczowski, S. (1978) Synthesis of rare earth carbonates under hydrothermal conditions. *J. Crystal Growth*, **44**, 84–96.

Deans, T. and Roberts, B. (1984) Carbonatite tuffs and lava clasts of the Tinderet foothills, Western Kenya: a study of calcified natrocarbonatites. *Proc. Geol. Soc. London*, **141**, 563–80.

—— and Seager, A. F. (1978) Stratiform magnetite crystals of abnormal morphology from volcanic carbonatites in Tanzania, Kenya, Greenland and India. *Mineral. Mag.*, **42**, 463–75.

Goldschmidt, V. M. (1958) *Geochemistry*. Oxford University Press, Oxford.

Jones, A. P. (1985) Carbonatite volcanics and geology of the Qagssiarssuk area, South Greenland: field notes to selected key localities. Unpublished field notes.

—— and Wyllie, P. J. (1985) Solubility of rare earth elements in carbonatite magmas, indicated by the liquidus surface in $CaCO_3$–$Ca(OH)_2$–$La(OH)_3$ at 1 kbar pressure. *Appl. Geochem.*, **1**, 95–102.

Keller, J. (1989) Extrusive carbonatites and their significance. In *Carbonatites* (Bell, K., ed.). Unwin Hyman, London, 70–88.

Knudsen, D. (1986) *Apatite mineralisation in carbona-tite and ultramafic intrusions in Greenland. Final report*. The Geological Survey of Greenland. 176 pp.

Kosterin, A. V. (1959) Possible modes of transport of the rare earths by hydrothermal solutions. *Geo-chemistry*, **4**, 381–7.

Mariano, A. N. (1988) Some further geological appli-cations of cathodoluminescence. In *Cathodolumi-nescence of Geological Materials* (Marshall, D. J., ed.). Unwin and Allen Inc., Oxford. 94–123.

—— and Ring, P. J. (1975) Europium-activated catho-doluminescence in minerals. *Geochim. Cosmochim. Acta*, **39**, 649–60.

—— and Roedder, P. L. (1983) Kerimasi: a neglected carbonatite volcano. *J. Geol.*, **91**, 449–55.

Marshall, D. J. (1988) *Cathodoluminescence of Geo-logical Materials*. Unwin and Allen Inc. Oxford.

Nakamura, N. (1974) Determination of *REE*, Ba, Fe, Mg, Na and K in carbonaceous chondrites. *Geochim. Cosmochim. Acta*, **38**, 757–75.

Pierson, B. J. (1981) The control of cathodolumi-nescence in dolomite by iron and manganese. *Sedi-mentology*, **28**, 601–10.

Stewart, J. N. (1970) *Precambrian alkaline–ultramafic/ carbonatite volcanism at Qagssiarssuk, South Green-land*. Grønlands Geologiske Uder Søgelse. C. A. Rietzels Folog. Kopenhagen, Denmark.

Tuttle, O. F. and Gittins, J. (1966) *Carbonatites*. Wiley, New York. 591 pp.

Upton, B. G. J. and Emeleus, C. H. (1987) Mid-Proterozoic magmatism in Southern Greenland: the Gardar Province. In *Alkaline Igneous Rocks*. Geol. Soc. Special Publication, **30**, 449–71.

Woolley, A. R. and Kempe, D. R. C. (1989) Carbona-tites: nomenclature, average chemical compositions and element distributions. In *Carbonatites* (Bell, K., ed.). Unwin Hyman, London, 1–14.